Activation of calcium entry in human carcinoma A431 cells by store depletion and phospholipase C-dependent mechanisms converge on I_{CRAC}-like calcium channels

Elena Kaznacheyeva*, Alexander Zubov*, Konstantin Gusev*, Ilya Bezprozvanny†, and Galina N. Mozhayeva*‡

*Institute of Cytology RAS, 4 Tikhoretsky Avenue, St. Petersburg 194064, Russia; and †Department of Physiology, University of Texas Southwestern Medical Center, Dallas, TX 75390

Edited by Bertil Hille, University of Washington, Seattle, WA, and approved November 8, 2000 (received for review June 26, 2000)

Activation of phospholipase C in nonexcitable cells causes the release of calcium (Ca^{2+}) from intracellular stores and activation of Ca^{2+} influx by means of Ca^{2+} release-activated channels (I_{CRAC}) in the plasma membrane. The molecular identity and the mechanism of I_{CRAC} channel activation are poorly understood. Using the patch–clamp technique, here we describe the plasma membrane Ca^{2+} channels in human carcinoma A431 cells, which can be activated by extracellular UTP, by depletion of intracellular Ca^{2+} stores after exposure to the Ca^{2+}-pump inhibitor thapsigargin, or by loading the cells with Ca^{2+} chelator 1,2-bis(2-aminophenoxy)ethane-*N,N,N′,N′*-tetraacetate. The observed channels display the same conductance and gating properties as previously described I_{min} channels, but have significantly lower conductance for monovalent cations than the I_{CRAC} channels. Thus, we concluded that the depletion-activated Ca^{2+} current in A431 cells is supported by I_{CRAC}-like (I_{CRACL}) channels, identical to I_{min}. We further demonstrated synergism in activation of I_{CRACL} Ca^{2+} channels by extracellular UTP and intracellular inositol (1,4,5)-triphosphate (IP_3), apparently because of reduction in phosphatidylinositol 4,5-bisphosphate (PIP_2) levels in the patch. Prolonged exposure of patches to thapsigargin renders I_{CRACL} Ca^{2+} channels unresponsive to IP_3 but still available to activation by the combined action of IP_3 and anti-PIP_2 antibody. Based on these data, we concluded that phospholipase C-mediated and store-operated Ca^{2+} influx pathways in A431 cells converge on the same I_{CRACL} Ca^{2+} channel, which can be modulated by PIP_2.

Activation of phospholipase C (PLC)-mediated signaling pathways in nonexcitable cells causes the release of Ca^{2+} from intracellular Ca^{2+} stores and activation of Ca^{2+} influx across the plasma membrane by means of capacitative Ca^{2+} entry or store-operated Ca^{2+} entry processes (1–3). These processes are mediated by plasma membrane Ca^{2+} channels termed "Ca^{2+} release activated channels" (I_{CRAC}) (4–7). The molecular identity of I_{CRAC} remains unclear, with mammalian *trp* channels (mTrp) usually considered the most likely candidate for the role of I_{CRAC} (1–3, 8, 9). When compared with I_{CRAC}, mTrp channels display relatively low selectivity for divalent cations, higher single channel conductance, and different kinetic and pharmacological properties. In experiments with a human carcinoma A431 cell line, we previously described plasma membrane Ca^{2+} channels (I_{min}) that are activated by application of uridine triphosphate and bradykinin to cell-attached patches or by application of inositol (1,4,5)-trisphosphate (IP_3) to excised inside-out (i/o) patches (10–12). IP_3-gated channels that share some common properties with I_{min} have been also observed in experiments with human T cells (13), rat macrophages (12), and endothelial cells (14, 15). Major functional properties of I_{min} channels, such as small conductance (1 pS for divalent cations), high selectivity for divalent cations ($P_{Ca/K} > 1{,}000$), inward rectification, and sensitivity to block by SKF95365 are similar to I_{CRAC} channels (12, 16). Thus, we previously suggested that I_{min} and I_{CRAC} may in fact be the same channels (17).

The mechanism of I_{CRAC} activation remains similarly controversial (1–3). When studied in a heterologous expression system, activation of mTrp channels by IP_3 appear to be mediated by direct conformational coupling between the cytosolic carboxyl-terminal tail of mTrp and the amino-terminal ligand-binding domain of intracellular IP_3 receptor (IP_3R) (18–21). However, whether mTrp can serve as an appropriate model system for understanding I_{CRAC} activation is unresolved (18, 21, 22). In previous studies, we demonstrated that activity of I_{min} in i/o patches is potentiated by addition of IP_3R-enriched microsomes as predicted by an I_{min}-IP_3R conformational coupling model (16). More recently, we discovered that anti-PIP_2 antibody (PIP_2Ab) sensitizes I_{min} to IP_3 activation and proposed an I_{min}-IP_3R-PIP_2 functional coupling model based on these findings (17). In parallel with our results, a potential role of PIP_2 in *trp*-like (*trpl*) channel activation has been recently demonstrated in Sf9 cells (23). The I_{min}-IP_3R-PIP_2 coupling model can adequately explain activation of I_{min} channels by direct action of PLC but not the activation of I_{CRAC} channels resulting from Ca^{2+} store depletion (4–6).

A number of critical questions related to a depletion-activated Ca^{2+} influx pathway remain unanswered. Most importantly, do store-depletion and PLC-dependent pathways activate the same or a different channel type? To answer this question, we compare the effects of PLC-linked agonist UTP, Ca^{2+} pump inhibitor thapsigargin (Tg), and Ca^{2+} chelator 1,2-bis(2-aminophenoxy)ethane-*N,N,N′,N′*-tetraacetate (BAPTA) on plasma membrane Ca^{2+} channel activity in patch–clamp experiments performed with human carcinoma A431 cells. We conclude that PLC activation and depletion of intracellular Ca^{2+} stores activate the same Ca^{2+} channel in A431 cells. We found that the conductance and selectivity properties of the store-operated channel in A431 cells are identical to the properties of I_{min} and somewhat different from the properties of I_{CRAC} channels described in Jurkat T cells (5–7). Thus, we will refer to store-operated channels in A431 cells as I_{CRACL} ("crac-like"). We also concluded that PIP_2 plays a role in modulation of I_{CRACL} activity.

Materials and Methods

Electrophysiological Recordings. Human carcinoma A431 cells (Cell Culture Collection, Institute of Cytology, St. Petersburg,

This paper was submitted directly (Track II) to the PNAS office.

Abbreviations: PLC, phospholipase C; I_{CRAC}, Ca^{2+} release activated channel; I_{CRACL}, I_{CRAC}-like; IP_3, inositol 1,4,5-triphosphate; IP_3R, IP_3 receptor; PIP_2, phosphatidylinositol (1,4,5)-bisphosphate; c/a, cell-activated; i/o, inside-out; Tg, thapsigargin; BAPTA, 1,2-bis(2-aminophenoxy)ethane-*N,N,N′,N′*-tetraacetate.

‡To whom reprint requests should be addressed. E-mail: gnmozh@link.cytspb.rssi.ru.

The publication costs of this article were defrayed in part by page charge payment. This article must therefore be hereby marked "*advertisement*" in accordance with 18 U.S.C. §1734 solely to indicate this fact.

Russia) were kept in culture, as described elsewhere (12). For patch–clamp experiments, cells were seeded onto coverslips and maintained in culture for 1–3 days before use. Single-channel currents were recorded by using the cell-attached and i/o configuration of the patch–clamp technique (24). Currents filtered at 500 Hz were recorded with a PC-501A patch–clamp amplifier (Warner Instruments, Hamden, CT) with a conventional resistance feedback in the headstage (10 GΩ). The currents were digitized at 2.5 kHz. For data analysis and presentation, currents were additionally digitally filtered at 100 Hz.

NP_o was determined by using the following equation: $NP_o = \langle I \rangle / i$, where $\langle I \rangle$ and i are the mean channel current and unitary current amplitude, respectively. $\langle I \rangle$ was estimated from the time integral of the current above the baseline, and i was determined from current records and all-point amplitude histograms. Data were collected from current records after channel activity reached steady state. Because channel activity was transient and displayed significant fluctuations, we used NP_o collected during 30 s of maximal activity ($NP_o^{max}{}_{30}$) as a standard way to compare open channel probability among different experiments. Average $NP_o^{max}{}_{30}$ values of channel activity from several experiments are presented in the text and on the figures as mean ± SEM. The pipette solution contained (in mM): 105 $BaCl_2$, 105 $CaCl_2$, or 140 NaCl as indicated, and 10 Tris/HCl (pH 7.4). In cell-attached experiments, the bath solution contained 140 mM KCl and 2 mM $CaCl_2$ to nullify the cell's resting potential. For BAPTA-AM loading, 100 μM BAPTA-AM and 1 μM Tg were added to the bath solution containing (in mM): 140 KCl, 5 NaCl, 10 Hepes/KOH, and 2 EGTA (pH 7.4). For i/o experiments, patches were excised into the standard intracellular solution containing (in mM): 140 K glutamate, 5 NaCl, 1 $MgCl_2$, 10 Hepes/KOH, 1.13 $CaCl_2$, and 2 EGTA (pCa 7, pH 7.4), with or without IP_3 as indicated. The cell-attached and i/o recordings were performed at −70 mV holding potential. All experiments were carried out at room temperature (22–24°C).

Materials. Monoclonal anti-PIP_2 antibody (PIP_2Ab) (25) was from PerSeptive Biosystems (Framingham, MA), and monoclonal anti-PIP antibody (PIPAb) was from Assay Designs (Ann Arbor, MI). PIP_2Ab and PIPAb were reconstituted in PBS (titer 1:1,500), diluted 1:100 by intracellular solution and used for chamber perfusion. Hepes, UTP, and Tg were from Sigma; EGTA was from Fluka Chemie AG (Buchs, Switzerland). IP_3 and BAPTA-AM were from Calbiochem.

Results

Exposure to Extracellular UTP Sensitizes I_{min} to IP_3 Activation. When cell-attached (c/a) recordings of I_{min} in A431 cells were performed in control recording conditions, the channel activity was very low with $NP_o^{max}{}_{30}$ equal to 0.08 ± 0.06 (n = 12) (Fig. 1 *a* and *c*). After patch excision in bath solution containing 2.5 μM IP_3, moderate activity of I_{min} in i/o patches was observed with $NP_o^{max}{}_{30}$ equal to 0.86 ± 0.2 (n = 12) (Fig. 1 *a* and *c*). Similar behavior of I_{min} channels in c/a and i/o configurations has been described (10–12, 17). As we previously reported, addition of 100 μM UTP or 10 μM bradykinin to the solution bathing A431 cells leads to activation of PLC-coupled receptors and an increase in I_{min} activity in c/a patches to $NP_o^{max}{}_{30}$ of 0.7–1.0 (12). When 100 μM UTP was included in the pipette solution, significantly higher I_{min} channel activity was observed with $NP_o^{max}{}_{30}$ equal to 1.5 ± 0.17 (n = 33) (Fig. 1*b*). With either bath (12) or pipette (Fig. 1*b*) UTP application, activity of I_{min} was transient and resulted in channel inactivation within several minutes. After patch excision into intracellular solution containing 2.5 μM IP_3, very high levels of I_{min} channel activity were observed (Fig. 1*b*). On an average, I_{min} channel $NP_o^{max}{}_{30}$ increased from 1.31 + 0.17 (c/a) to 2.91 + 0.23 (i/o) in this series of experiments (n = 9) following patch excision (Fig. 1*c*).

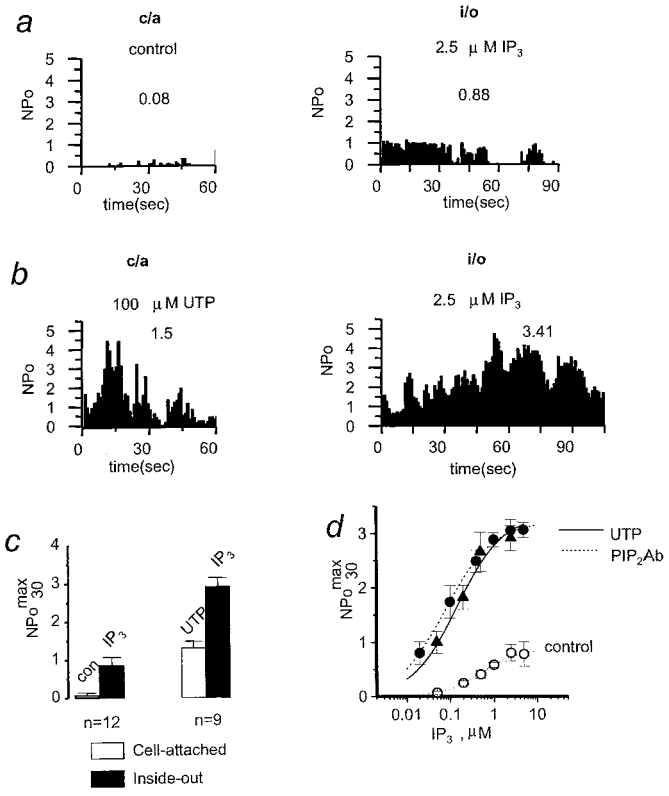

Fig. 1. Sensitization of I_{min} to IP_3 by extracellular UTP. (*a*) Plot of I_{min} open channel probability (NP_o) in cell-attached (c/a) patch recorded in control conditions and in i/o patch from the same cell in the presence of 2.5 μM IP_3. The NP_o was averaged over 1-s intervals and plotted vs. time in the experiment. Mean $NP_o^{max}{}_{30}$ was 0.08 in c/a and 0.88 in i/o for the experiment shown. Data are representative of 12 experiments. (*b*) Same plot as in *a* for the experiment with 100 μM UTP in the pipette. Mean $NP_o^{max}{}_{30}$ was 1.5 in c/a and 3.41 in i/o for the experiment shown. Data are representative of nine experiments. (*c*) The summary plot of I_{min} open channel probability in c/a (open bars) and i/o (closed bars) recordings performed in control conditions (n = 12, left) or in the presence of 100 μM UTP in the pipette (n = 9, right). I_{min} activity is represented as $NP_o^{max}{}_{30}$ (mean ± SEM). (*d*) $NP_o^{max}{}_{30}$ of I_{min} channels in i/o experiments at IP_3 concentrations as indicated measured with 100 μM UTP in the pipette (▲), in the presence of PIP_2Ab (●) and in control conditions (○). Average data at each IP_3 concentration are shown as mean ± SEM ($n \geq 6$). Smooth curve, best fit the data obtained with UTP in the pipette by using the equation $NP_o^{max}{}_{30} = (NP_o^{max}{}_{30})^{max} [IP_3]^{nH} / ([IP_3]^{nH} + K_{app}{}^{nH})$, the values of parameters are in the text. Dashed lines, fit to the similar data obtained in control conditions (curve on the right) and in the presence of PIP_2Ab (curve on the left). The data for control conditions and in the presence of PIP_2Ab are taken from ref. 17.

To gain insight into the mechanism responsible for the unusually high activity of I_{min} channels in i/o recordings observed in the experiments with UTP in the pipette (Fig. 1 *b* and *c*), we determined the sensitivity of I_{min} activation by IP_3 when 100 μM of UTP was included in the pipette solution. In all experiments of this series, we waited until I_{min} activity in c/a patches subsided before the patch excision. A single IP_3 concentration in the 0.05–2.5 μM range was tested in each experiment to avoid IP_3-induced I_{min} desensitization (12). Fitting the Hill equation to the data (Fig. 1*d*, ▲) yielded an apparent affinity (K_{app}) of 0.15 μM IP_3, maximal $NP_o^{max}{}_{30}$ (NP_o^{max}) of 3.33, and a Hill coefficient (n_H) of 0.83 (Fig. 1*d*, curve). When similar experiments were performed in control recording conditions, sensitivity of I_{min} to IP_3 activation was much lower (K_{app} = 0.51 μM IP_3, NP_o^{max} = 0.87, n_H = of 1.05) (17) (Fig. 1*d*, ○, and dashed line on the right). The dramatic increase in I_{min} apparent affinity for IP_3 and in NP_o^{max} induced by exposure to UTP in the pipette

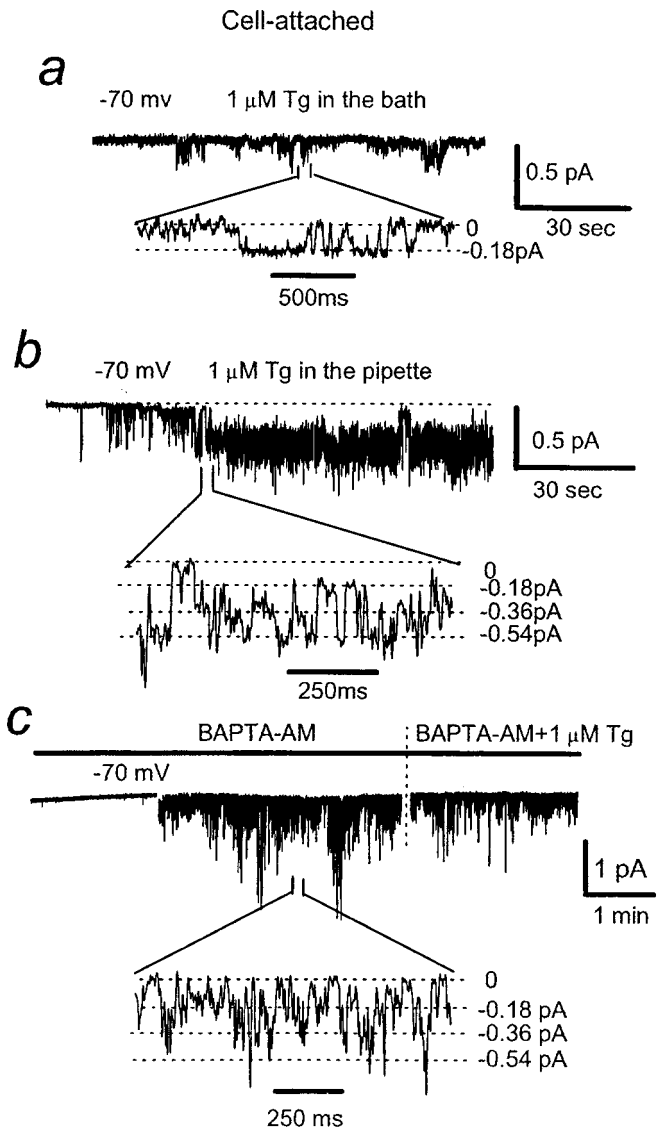

Fig. 2. Activation of I_{min} channels by Tg. (*a*) Ca^{2+} channel current traces in c/a patches recorded in the presence of 1 μM Tg in the bath solution. The fragments of current records are shown on the bottom on expanded time scale. The unitary current amplitude in used recording conditions (−70 mV membrane resting potential) is −0.18 pA. (*b*) Same as in *a* with 1 μM Tg in the pipette. (*c*) Same as in *a* with 100 μM BAPTA-AM and 1 μM Tg in the bath.

quantitatively matches with the effects exerted by PIP_2Ab on I_{min} (K_{app} = 0.08 μM IP_3, NP_o^{max} = 3.21, n_H = of 0.8) (17) (Fig. 1*d*, ●, and dashed line on the left) and on the IP_3R (26). We reasoned that synergistic actions of extracellular UTP and intracellular IP_3 in our experiments (Fig. 1) result from UTP receptor stimulation of PLC which decreases PIP_2 levels in the patch. Reduction of PIP_2 levels leads to an increase in the apparent affinity of IP_3R for IP_3 (26) and in the potency of IP_3 to activate I_{min}.

I_{min} Is the I_{CRACL} Channel Activated by Depletion of Intracellular Ca^{2+} Stores. I_{CRAC} currents can be activated in cells without PLC activation as a result of intracellular Ca^{2+} store depletion following exposure to Ca^{2+}-ATPase inhibitor Tg or intracellular Ca^{2+} chelators BAPTA and EGTA (4, 5). The experiments described in the previous section support the I_{min}-IP_3R-PIP_2 coupling model (17). This model explains activation of I_{min} channels by direct action of PLC but not the activation of I_{CRAC} channels by Ca^{2+} store depletion. Does depletion of Ca^{2+} stores activate the same channel as activation of PLC? To answer this question, we evaluated effects of Tg on Ca^{2+} channel activity in patch–clamp experiments. As in our previous studies (12), addition of 1 μM Tg to the bath had only minimal effect on I_{min} activity when compared with control conditions, with $NP_o^{max}{}_{30}$ equal to 0.11 ± 0.03 (n = 9) (Fig. 2*a*; also see Fig. 4 *a* and *h*). In contrast to these results, if 1 μM Tg was included in the pipette, active I_{min} channels were observed following a short delay after patch formation, with $NP_o^{max}{}_{30}$ equal to 1.7 ± 0.24 (n = 18) (Figs. 2*b* and 4 *b* and *h*). We interpret this delay as the time needed for depletion of submembrane Ca^{2+} stores by Tg entering the cell from the pipette.

One potential explanation of different effects caused by bath and pipette applications of Tg is Ca^{2+}-induced inactivation of I_{min}. From comparison of I_{min} rundown kinetic with Ca^{2+} or Ba^{2+} as a current carrier, we previously concluded that I_{min} is likely to undergo Ca^{2+}-induced inactivation process (11). Massive Ca^{2+} release from the stores resulting from bath application of Tg may quickly inactivate I_{min}, but if Tg is included only in the pipette, Ca^{2+} leak is much slower, and I_{min} inactivation may be reduced or decelerated. To test this hypothesis, we clamped Ca^{2+} concentration in A431 cells by loading them with the membrane-permeable Ca^{2+} chelator BAPTA-AM. Bath application of 0.1 mM BAPTA-AM by itself resulted in I_{min} activity in 9 of 15 experiments. In six remaining experiments, application of Tg to BAPTA-loaded cells evoked I_{min} channel activity. To simplify experimental procedure, we combined application of Tg and BAPTA-AM to the bath, which resulted in I_{min} channel activity in 7 of 10 experiments (Figs. 2*c* and 4*c*). From these results, we concluded that the low potency of Tg in the bath to activate I_{min} in our previous experiments (Fig. 2*a*) (12) mostly likely results from Ca^{2+}-dependent inactivation of I_{min}.

Activation of I_{min} by depletion of intracellular Ca^{2+} stores with

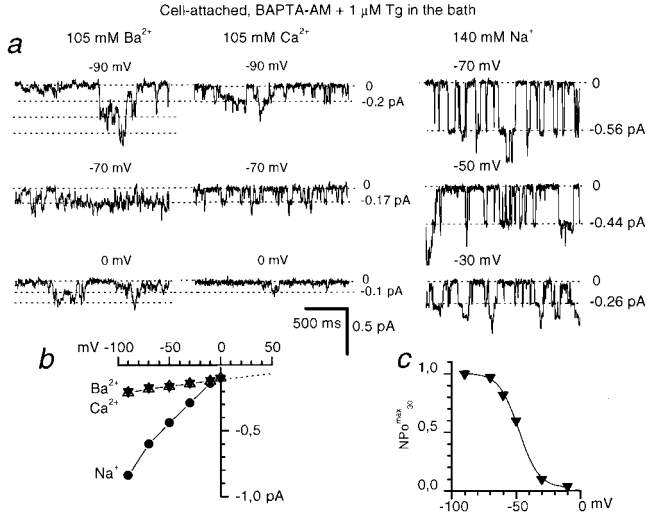

Fig. 3. Conductance properties of store-operated channels in A431 cells. (*a*) Store-operated channels in A431 cells, activated by the mixture of 100 μM BAPTA-AM and 1 μM Tg in the bath solution, were recorded in c/a mode with 105 mM Ba^{2+} (*Left*), 105 mM Ca^{2+} (*Center*), and 140 mM Na^+ (*Right*) in the pipette solution at membrane potential as indicated. (*b*) Fit to the unitary current-voltage relationship of store-operated channels with Ba^{2+} (▼, n = 4–6), Ca^{2+} (△, n = 4), Na^+ (●, n = 3) yielded slope single-channel conductance of 1 pS for Ca^{2+} and Ba^{2+} and 6 pS for Na^+. (*c*) Open channel probability of store-operated channels ($NP_o^{max}{}_{30}$) expressed as a function of membrane potential. Data from six independent experiments in c/a mode with 105 mM Ba^{2+} as a current carrier were averaged at each membrane potential (▼). (*b* and *c*) The average values are shown as mean ± SEM, unless the size of the error bars is smaller than the size of the symbols.

Tg and BAPTA-AM (Fig. 2 *b* and *c*) reinforces the idea that I_{min} and I_{CRAC} may in fact be the same channels (17). To test this idea further and in the absence of molecular information and specific blockers, we resorted to comparison of I_{min} and I_{CRAC} single-channel properties. The divalent single-channel conductance of I_{CRAC} channels in Jurkat T cells has been estimated to be 24 fS from the noise analysis (6), and the monovalent single-channel conductance has been measured at 40 pS with Na^+ as a current carrier (7). It has also been demonstrated that the permeability of I_{CRAC} to Ca^{2+} is higher than for Ba^{2+} (6, 27). With 105 mM divalent cations in the pipette, the store-operated channels in A431 cells were equally permeable to Ca^{2+} and Ba^{2+} (Fig. 3), displayed a single-channel current amplitude of −0.18 pA at −70 mV membrane potential (Figs. 2 and 3) and a single-channel conductance of about 1 pS (Fig. 3). Thus, conductance properties of these channels are identical to the properties of I_{min} channels activated by UTP (in c/a) or by IP_3 (in i/o) (12). We also demonstrated that the open probability of store-operated channels in A431 cells is strongly dependent on the membrane potential (Fig. 3), in line with the properties of I_{min} (12). Using 140 mM Na^+ as a current carrier, we determined that store-depletion activated channels in A431 cells displayed the main conductance level of −0.56 pA at −70 mV membrane potential and the corresponding single channel conductance of 6 pS (Fig. 3), which is several-fold smaller than conductance of I_{CRAC} channels in Jurkat T cells in similar ionic conditions (7). From these results, we concluded that the store-depletion activated Ca^{2+} current in A431 is carried by I_{CRAC}-like (I_{CRACL}) channels, which are identical to the previously described I_{min} channels (12). In the remaining section of the paper, these channels will be referred to simply as I_{CRACL}.

PIP_2 Is a Modulator of I_{CRACL}. When activated by UTP (Fig. 1*b*) or Tg (Fig. 4*b*), I_{CRACL} channel activity was transient, with channels typically lasting between 2 and 5 min. Loading of A431 cells with BAPTA-AM dramatically extended the period of Tg-induced

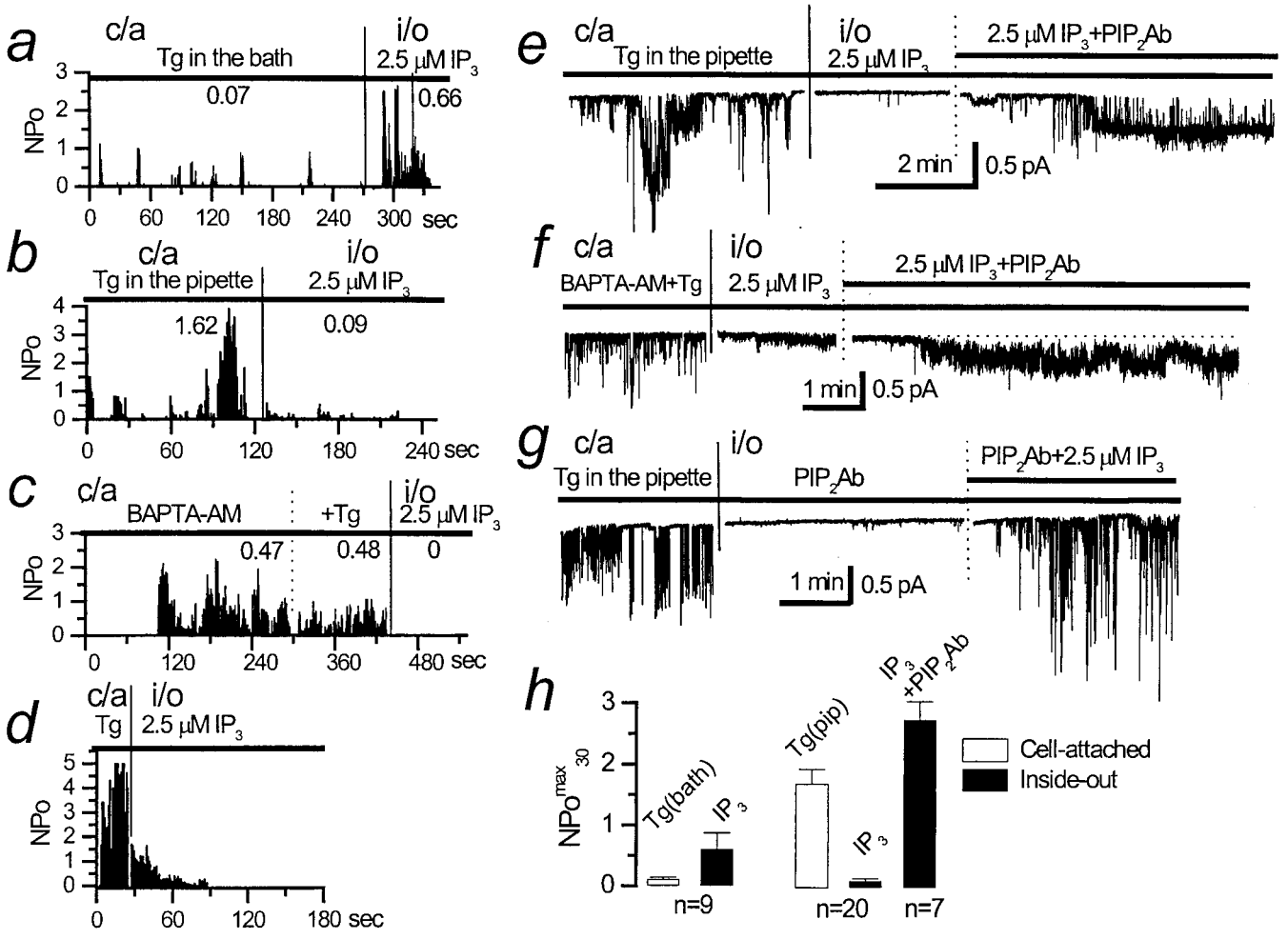

Fig. 4. Role of PIP_2 in I_{CRACL} modulation. (*a*) Plot of I_{CRACL} open channel probability (NP_o) in c/a patch recorded with 1 μM Tg in the bath and in i/o patch from the same cell in the presence of 2.5 μM IP_3. The NP_O was averaged over 1-s intervals and plotted vs. time in the experiment. Mean $NP_o^{max}{}_{30}$ was 0.07 in c/a and 0.66 in i/o for the experiment shown. Data are representative of nine experiments. (*b*) Same plot as in *a* for the experiment with 1 μM Tg in the pipette. Mean $NP_o^{max}{}_{30}$ was 1.62 in c/a and 0.09 in i/o for the experiment shown. Data are representative of 20 experiments. (*c*) Same plot as in *a* for the experiment with 100 μM BAPTA-AM and 1 μM Tg in the bath. Mean $NP_o^{max}{}_{30}$ was 0.48 in c/a and 0 in i/o for the experiment shown. Data are representative of nine experiments. (*d*) Same plot as in *b*, but with patch excision within 30 s after I_{CRACL} activation. Data are representative of four experiments. (*e*) I_{CRACL} channel current traces in c/a patches recorded in the presence of 1 μM Tg in the pipette solution followed by i/o current recordings in the presence of 2.5 μM IP_3 and PIP_2Ab as shown. Data are representative of seven experiments. (*f*) Same as in *e* with 100 μM BAPTA-AM and 1 μM Tg in the bath. Data are representative of four experiments. (*g*) Same as in *e* with the order of PIP_2Ab and IP_3 additions to i/o patch reversed. Data are representative of five experiments. (*h*) The summary plot of I_{CRACL} open channel probability in c/a (open bars) and i/o (closed bars) recordings performed in the presence of 1 μM Tg in the bath ($n = 9$, left) or in the presence of 1 μM Tg in the pipette ($n = 20$, right). I_{CRACL} activity is represented as $NP_o^{max}{}_{30}$ (mean ± SEM).

I_{CRACL} activity, effectively preventing I_{CRACL} inactivation (Fig. 4*c*). Thus, we concluded that the Ca^{2+}-dependent mechanism plays a major role in I_{CRACL} inactivation, similar to the previous studies of I_{CRAC} (27, 28). To get additional insight into the mechanisms of I_{CRACL} inactivation, we evaluated responses of I_{CRACL} channels to IP_3 in i/o patches. With 1 μM Tg in the bath, normal activation of I_{CRACL} channels by 2.5 μM IP_3 was observed in i/o patches (Fig. 4 *a* and *h*), similar to control experiments (Fig. 1*a*). However, exposure to 1 μM Tg in the pipette, which initially resulted in I_{CRACL} activation, eventually led to channel inactivation and greatly diminished activity of IP_3-gated I_{CRACL} channels in i/o mode (Fig. 4*b*). On average, I_{CRACL} channel activity in i/o patches with Tg in the pipette was reduced to $NP_o{}^{max}{}_{30}$ equal to 0.11 $\pm$ 0.03 (n = 20) (Fig. 4*h*). Tg-induced loss of I_{CRACL} channel sensitivity to activation by IP_3 developed in time. Indeed, when patches were excised within 30 s from the initial channel activation, substantial I_{CRACL} channel activity in i/o patches was initially observed in the presence of 2.5 μM IP_3 in 1 of 4 experiments (Fig. 4*d*). Although loading the cells with BAPTA-AM almost completely removed I_{CRACL} inactivation in c/a mode (Fig. 4*c*), the channels in these experiments were also unresponsive to IP_3 in i/o mode (Fig. 4*c*). Thus, following exposure to Tg, patch excision lead to a loss of I_{CRACL} responsiveness to IP_3, even in the absence of Ca^{2+}-dependent inactivation.

Inclusion of UTP in the pipette resulted in sensitization of I_{CRACL} channels to IP_3 (Fig. 1 *c* and *d*), which we concluded was related to PLC-dependent reduction in PIP_2 levels in the patch (see above). What if depletion of Ca^{2+} stores, which leads to a loss of I_{CRACL} sensitivity to IP_3 in i/o patches (Fig. 4 *b–d* and *h*), increases the fraction of PIP_2-tethered IP_3R-I_{CRACL} complexes? To test this hypothesis, we analyzed the effect of PIP_2Ab on I_{CRACL} in i/o patches taken from cells exposed to Tg in the pipette or to the BAPTA-AM/Tg mixture in the bath. Although I_{CRACL} was rendered sensitive to IP_3 as a result of prolonged patch exposure to Tg, addition of PIP_2Ab restored I_{CRACL} channel activity (Fig. 4*e*), with $NP_o{}^{max}{}_{30}$ = 2.73 $\pm$ 0.3 (n = 7) (Fig. 4*h*). Similar results were obtained in the experiments (n = 4) where I_{CRACL} channels were initially activated by a BAPTA-AM/Tg mixture in the bath (Fig. 4*f*). The observed effect was specific for PIP_2Ab, as addition of PIPAb had no effect on I_{CRACL} channel activity in control experiments (n = 5). Similar to our previous results (17), PIP_2Ab alone did not induce channel activity in these conditions, but instead greatly potentiated the ability of IP_3 to activate the I_{CRACL} (Fig. 4*g*). The experiments with PIP_2Ab support the hypothesis that, following exposure to Tg and store-depletion, all I_{CRACL}-IP_3R complexes in the patch are shifted to the PIP_2-tethered state. In the absence of Ca^{2+}-induced inactivation, I_{CRACL} channels in I_{CRACL}-IP_3R-PIP_2 complexes remain active as long as store is depleted but do not respond to IP_3.

Discussion

PLC-Dependent and Store-Operated Pathways of I_{CRACL} Activation. Our results lead us to conclude that both PLC-linked and Ca^{2+} store-operated Ca^{2+} entry pathways in A431 cells are in fact supported by the same Ca^{2+} channel, with single-channel properties identical to the properties of the previously described I_{min} channel (12). Similar to I_{min}, the store-operated channels in A431 cells are equally permeable to Ca^{2+} and Ba^{2+} and display a divalent single channel conductance of 1 pS. Monovalent single-channel conductance of these channels is 5.5–6 pS with 140 mM Na^+ as a current carrier, which is several-fold smaller than single-channel conductance of I_{CRAC} channels in Jurkat T cells measured in similar ionic conditions (40 pS) (7). To account for the observed differences in conductance and selectivity properties, we called the store-operated channel in A431 cells I_{CRACL} (I_{CRAC}-like). Ca^{2+} channels activated by depletion of intracellular stores in A431 cells were previously described (29). However, these channels are clearly distinct from I_{CRACL} as they display higher permeability to Ba^{2+} than to Ca^{2+} (16 pS at 160 mM Ba^{2+} and 2 pS at 200 mM Ca^{2+}), not permeable to Na^+, not voltage-dependent, and do not respond to IP_3 in i/o patches (29). Therefore, these channels constitute an alternative depletion-activated Ca^{2+} influx pathway in A431 cells. We have not observed channels described by Luckhoff and Clapham (29) in our experiments, most likely because of variability between different A431 clones or effects of culture conditions on channel expression. In some patches on A431 cells, we observed nonselective cation permeable channels with large conductance, which were clearly distinct from the I_{CRACL}. These channels did not respond to IP_3 or Tg, and the patches containing these channels were discarded.

What is a mechanism of I_{CRACL} activation? From the present results and from our previous work on I_{min}, we conclude that I_{CRACL} channels in A431 cells are conformationally coupled to intracellular IP_3R and can be activated: (*i*) by changes in the IP_3R receptor conformation on IP_3 binding (16); (*ii*) by direct cleavage of I_{CRACL}-IP_3R-tethered PIP_2 by PLC (17); and (*iii*) by the store-operated mechanism as in the conformational coupling mechanism originally proposed by Irvine (ref. 30) (present results). Gating of I_{CRACL}-IP_3R complexes by IP_3 probably accounts for the low background channel activity in resting cells (Fig. 1*a*) (endogenous IP_3 level is estimated at 40–100 nM in unstimulated cells; ref. 31), and for the substantial activity of I_{CRACL} channels in excised patches in the

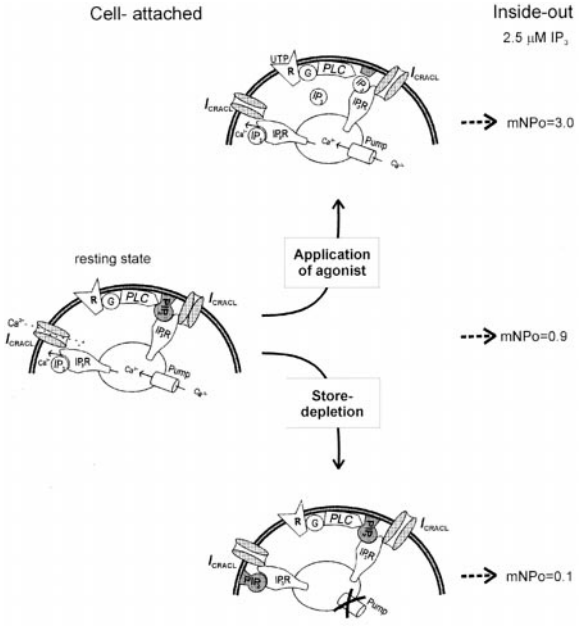

Fig. 5. Model of I_{CRACL} conformational coupling to IP_3R and modulation by PIP_2. I_{CRACL}-IP_3R and I_{CRACL}-IP_3R-PIP_2 complexes exist in equilibrium in resting cells (*Left*). Background I_{CRACL} channel activity in cell-attached patches in resting cells results from endogenous IP_3 (40–100 nM) (31) activating I_{CRACL}-IP_3R complexes. Exposure of patches excised from the resting cells to 2.5 μM IP_3 leads to elevated I_{CRACL} channel activity in i/o configuration (*Right*). Exposure to UTP in the pipette triggers cleavage of IP_3R-tethered PIP_2 and direct activation of I_{CRACL}-IP_3R-PIP_2 complexes in cell-attached patches as previously proposed (17). The shift from I_{CRACL}-IP_3R-PIP_2 to I_{CRACL}-IP_3R complexes (*Top*) explains high activity of I_{CRACL} channels in i/o patches in the presence of 2.5 μM IP_3 (*Top Right*). Exposure to Tg in the pipette or to BAPTA-AM/Tg in the bath causes depletion of local Ca^{2+} stores and activation of I_{CRACL} channels by means of conformational coupling mechanism (30). Depletion of Ca^{2+} stores by some unknown mechanism promotes formation of I_{CRACL}-IP_3R-PIP_2 complexes (*Bottom*), which leads to the loss of I_{CRACL} sensitivity to activation by 2.5 μM IP_3 in excised patches (*Bottom Right*). Despite loss of sensitivity to activation by IP_3, I_{CRACL} channels in I_{CRACL}-IP_3R-PIP_2 complexes remain active as long as stores are depleted and I_{CRACL} inactivation is prevented by chelating Ca^{2+} with BAPTA. The model drawing is adapted from ref. 47.

presence of 2.5 μM IP_3 (Fig. 1*a*). Cleavage of IP_3R-tethered PIP_2 by PLC is likely to be responsible for activation of I_{CRACL} channels by UTP in the pipette in our experiments (Fig. 1*b*). The activation of I_{CRACL} channels by Tg in the pipette (Fig. 2*b*) and by BAPTA-AM/Tg in the bath (Fig. 2*c*) results from the IP_3R conformational changes on intracellular Ca^{2+} store depletion. In physiological conditions, stimulation of cells by agonist leads to PLC activation, increase in IP_3 levels, and depletion of Ca^{2+} stores. Therefore, an additive or even synergistic action of three different pathways of I_{CRACL} activation in cells is expected in response to application of agonist *in situ*. Similar to I_{CRAC} (27, 28), I_{CRACL} channels are under strong negative inhibitory control by cytosolic Ca^{2+}, which normally leads to a transient nature of I_{CRACL} activity (Figs. 1*b* and 4*b*). Loading A431 cells with BAPTA removes Ca^{2+}-dependent inactivation and dramatically increases the duration of I_{CRACL} activity (Fig. 4*c*).

Role of PIP_2 as a Modulator of I_{CRACL} Channels. Our data also suggest that PIP_2 may play a role of I_{CRACL} modulator by regulating a dynamic equilibrium between I_{CRACL}-IP_3R and I_{CRACL}-IP_3R-PIP_2 complexes (Fig. 5 *Left*). Following exposure to UTP, activation of PLC and cleavage of PIP_2 in the patch, the majority of I_{CRACL} channels are shifted to PIP_2-free I_{CRACL}-IP_3R state (Fig. 5 *Top*), as manifested by $NP_o^{max}{}_{30} = 3$ in i/o patches with 2.5 μM IP_3 in these experiments (Fig. 5 *Top Right*) compared with $NP_o^{max}{}_{30} = 0.86$ in control patches (Fig. 5 *Right*). Depletion of the stores with Tg or BAPTA appears to shift the equilibrium in the opposite direction, with all of I_{CRACL} channels driven to I_{CRACL}-IP_3R-PIP_2 complexes (Fig. 5 *Bottom*). I_{CRACL} channels in these experiments were unresponsive to IP_3 in i/o patches with $NP_o^{max}{}_{30} = 0.1$ (Fig. 5 *Bottom Right*) but responded essentially at the maximal level ($NP_o^{max}{}_{30} = 2.7$) to a combination of 2.5 μM IP_3 and PIP_2Ab (Fig. 4*d*). Despite loss of sensitivity to activation by IP_3, I_{CRACL} channels in I_{CRACL}-IP_3R-PIP_2 complexes remain active in c/a mode (but not in i/o mode, for reasons that need to be further investigated) as long as stores are depleted and I_{CRACL} inactivation is prevented by chelating Ca^{2+} (Fig. 4*c*). Possible mechanisms responsible for the store-dependent shift toward a PIP_2-occupied state of the IP_3R may include physical rearrangement of mobile Ca^{2+} stores (32), changes in local PIP_2 levels in the patch (33), or an increase in IP_3R affinity for PIP_2 following Ca^{2+} stores depletion. Additional experiments will be needed to discriminate between these possibilities.

Conformational Coupling Model of I_{CRACL} Activation. I_{CRACL}-IP_3R association is likely to involve direct binding of the IP_3R amino-terminal region to the I_{CRACL} protein, similar to mTrp-IP_3R association (21). Interestingly, the same amino-terminal region of IP_3R also includes specific IP_3 (34, 35) and PIP_2 (36) binding sites. Thus, ligand-induced conformational changes of the IP_3R amino-terminal region can be transmitted directly to the I_{CRACL} channel. The store-operated I_{CRACL} activation is likely to involve an IP_3R-associatied endoplasmic reticulum resident Ca^{2+}-binding protein, such as calreticulin (37–39), which serves as a sensor of intraluminal Ca^{2+}. Additional signaling components are likely to be recruited to the I_{CRACL}-IP_3R complex via actions of a modular adaptor protein, such as mGluR1/IP_3R-binding protein Homer in neuronal cells (40), the Syk/Btk/Grb2/PLCγ-binding protein BLNK in B lymphocytes (41), or the *trp*/PKC/PLC-binding protein *inaD* in *Drosophila* photoreceptors (42). The actin cytoskeleton may also play an important role in correct spatial arrangement of required signaling components (43–45). In chicken B lymphocytes, removal of all three IP_3R isoforms by genetic means had no effect on Tg-induced Ca^{2+} influx (46), in apparent conflict with the conformational coupling model of I_{CRACL} activation in A431 cells (Fig. 5). From these results, we conclude that the B lymphocytes must have an additional or alternative Ca^{2+} influx pathway, coupled to Ca^{2+} store depletion by means of IP_3R-independent mechanism that may involve a global "diffusible messenger." Additional functional studies with B lymphocytes will be required for its detailed characterization.

We thank V. A. Alexeenko for technical assistance, Phyllis Foley for help with preparation of the manuscript, and Dr. Bertil Hille for comments on the paper. This work is supported by the Russian Basic Research Foundation 98-04-49512 (to G.N.M), the National Institutes of Health NS38082 (to I.B.), and the Civilian Research and Development Foundation RB1-2018 (G.N.M. and I.B.).

1. Berridge, M. J. (1995) *Biochem. J.* **312,** 1–11.
2. Parekh, A. B. & Penner, R. (1997) *Physiol. Rev.* **77,** 901–930.
3. Putney, J. W., Jr., & McKay, R. R. (1999) *BioEssays* **21,** 38–46.
4. Hoth, M. & Penner, R. (1992) *Nature (London)* **355,** 353–356.
5. Premack, B. A., McDonald, T. V. & Gardner, P. (1994) *J. Immunol.* **152,** 5226–5240.
6. Zweifach, A. & Lewis, R. S. (1993) *Proc. Natl. Acad. Sci. USA* **90,** 6295–6299.
7. Kerschbaum, H. H. & Cahalan, M. D. (1999) *Science* **283,** 836–839.
8. Clapham, D. E. (1996) *Neuron* **16,** 1069–1072.
9. Birnbaumer, L., Zhu, X., Jiang, M., Boulay, G., Peyton, M., Vannier, B., Brown, D., Platano, D., Sadeghi, H., Stefani, E. & Birnbaumer, M. (1996) *Proc. Natl. Acad. Sci. USA* **93,** 15195–15202.
10. Mozhayeva, G. N., Naumov, A. P. & Kuryshev, Y. A. (1990) *FEBS Lett.* **277,** 233–234.
11. Kiselyov, K. I., Mamin, A. G., Semyonova, S. B. & Mozhayeva, G. N. (1997) *FEBS Lett.* **407,** 309–312.
12. Kiselyov, K. I., Semyonova, S. B., Mamin, A. G. & Mozhayeva, G. N. (1999) *Pflugers Arch.* **437,** 305–314.
13. Kuno, M. & Gardner, P. (1987) *Nature (London)* **326,** 301–304.
14. Luckhoff, A. & Clapham, D. E. (1992) *Nature (London)* **355,** 356–358.
15. Vaca, L. & Kunze, D. L. (1995) *Am. J. Physiol.* **269,** C733—C738.
16. Zubov, A. I., Kaznacheeva, E. V., Nikolaev, A. V., Alexeenko, V. A., Kiselyov, K., Muallem, S. & Mozhayeva, G. N. (1999) *J. Biol. Chem.* **274,** 25983–25985.
17. Kaznacheyeva, E., Zubov, A. N., Nikolaev, A., Alexeenko, V., Bezprozvanny, I. & Mozhayeva, G. N. (2000) *J. Biol. Chem.* **275,** 4561–4564.
18. Kiselyov, K., Xu, X., Mozhayeva, G., Kuo, T., Pessah, I., Mignery, G., Zhu, X., Birnbaumer, L. & Muallem, S. (1998) *Nature (London)* **396,** 478–482.
19. Kiselyov, K., Mignery, G. A., Zhu, M. X. & Muallem, S. (1999) *Mol. Cell* **4,** 423–429.
20. Vannier, B., Peyton, M., Boulay, G., Brown, D., Qin, N., Jiang, M., Zhu, X. & Birnbaumer, L. (1999) *Proc. Natl. Acad. Sci. USA* **96,** 2060–2064.
21. Boulay, G., Brown, D. M., Qin, N., Jiang, M., Dietrich, A., Zhu, M. X., Chen, Z., Birnbaumer, M., Mikoshiba, K. & Birnbaumer, L. (1999) *Proc. Natl. Acad. Sci. USA* **96,** 14955–14960.
22. Ma, H.-T., Patterson, R. L., Rossum, D. B., Birnbaumer, L., Mikoshiba, K. & Gill, D. L. (2000) *Science* **287,** 1647–1651.
23. Estacion, M., Sinkins, W. G. & Schilling, W. P. (2000) *J. Physiol. (London)*, in press.
24. Hamill, O. P., Marty, A., Neher, E., Sakmann, B. & Sigworth, F. J. (1981) *Pfluegers Arch.* **391,** 85–100.
25. Fukami, K., Matsuoka, K., Nakanishi, O., Yamakawa, A., Kawai, S. & Takenawa, T. (1988) *Proc. Natl. Acad. Sci. USA* **85,** 9057–9061.
26. Lupu, V. D., Kaznacheyeva, E., Krishna, U. M., Falck, J. R. & Bezprozvanny, I. (1998) *J. Biol. Chem.* **273,** 14067–14070.
27. Hoth, M. & Penner, R. (1993) *J. Physiol. (London)* **465,** 359–386.
28. Zweifach, A. & Lewis, R. S. (1995) *J. Gen. Physiol.* **105,** 209–226.
29. Luckhoff, A. & Clapham, D. E. (1994) *Biophys. J.* **67,** 177–182.
30. Irvine, R. F. (1990) *FEBS Lett.* **263,** 5–9.
31. Luzzi, V., Sims, C. E., Soughayer, J. S. & Allbritton, N. L. (1998) *J. Biol. Chem.* **273,** 28657–28662.
32. Yao, Y., Ferrer-Montiel, A. V., Montal, M. & Tsien, R. Y. (1999) *Cell* **98,** 475–485.
33. Raucher, D., Stauffer, T., Chen, W., Shen, K., Guo, S., York, J. D., Sheetz, M. P. & Meyer, T. (2000) *Cell* **100,** 221–228.
34. Mignery, G. A. & Sudhof, T. C. (1990) *EMBO J.* **9,** 3893–3898.
35. Miyawaki, A., Furuichi, T., Ryou, Y., Yoshikawa, S., Nakagawa, T., Saitoh, T. & Mikoshiba, K. (1991) *Proc. Natl. Acad. Sci. USA* **88,** 4911–4915.
36. Glouchankova, L., Krishna, U. M., Potter, B. V. L., Falck, J. R. & Bezprozvanny, I. (2000) *Mol. Cell Biol. Res. Comm.* **3,** 153–158.
37. Camacho, P. & Lechleiter, J. D. (1995) *Cell* **82,** 765–771.
38. Fadel, M. P., Dziak, E., Lo, C. M., Ferrier, J., Mesaeli, N., Michalak, M. & Opas, M. (1999) *J. Biol. Chem.* **274,** 15085–15094.
39. Michalak, M., Corbett, E. F., Mesaeli, N., Nakamura, K. & Opas, M. (1999) *Biochem. J.* **344,** 281–292.
40. Tu, J. C., Xiao, B., Yuan, J. P., Lanahan, A. A., Leoffert, K., Li, M., Linden, D. J. & Worley, P. F. (1998) *Neuron* **21,** 717–726.
41. Kurosaki, T. & Tsukada, S. (2000) *Immunity* **12,** 1–5.
42. Tsunoda, S., Sierralta, J., Sun, Y., Bodner, R., Suzuki, E., Becker, A., Socolich, M. & Zuker, C. S. (1997) *Nature (London)* **388,** 243–249.
43. Rossier, M. F., Bird, G. S. J. & Putney, J. W. J. (1991) *Biochem. J.* **274,** 643–650.
44. Holda, J. R. & Blatter, L. A. (1997) *FEBS Lett.* **403,** 191–196.
45. Ribeiro, C. M., Reece, J. & Putney, J. W., Jr. *(1997) J. Biol. Chem.* **272,** 26555–26561.
46. Sugawara, H., Kurosaki, M., Takata, M. & Kurosaki, T. (1997) *EMBO J.* **16,** 3078–3088.
47. Putney, J. W., Jr. (1999) *Proc. Natl. Acad. Sci. USA* **96,** 14669–14671.